JOURNAL OF RAMAN SPECTROSCOPY
J. Raman Spectrosc. 2001; **32**: 847–851

Pressure dependence of photoluminescence of $ZnTe/Zn_{1-x}Cd_xTe$ strained-layer superlattice

W. S. Li,[1,2] Z. X. Shen,[1]* H. Y. Li,[3] D. Z. Shen[3] and X. W. Fan[3]

[1]Department of Physics, Faculty of Science, National University of Singapore, 2 Science Drive 3, Singapore 117542.
[2]Technology Development, Chartered Semiconductor Mfg Ltd, 60 Woodlands Industrial Park D, Street 2, Singapore 738406
[3]Laboratory of Excited State Processes, Changchun Institute of Physics, Chinese Academy of Sciences, Changchun 130021, China

Received 13 September 2000; Accepted 29 May 2001

Photoluminescence (PL) spectra of $ZnTe/Zn_{1-x}Cd_xTe$ (x = 0.23) strained-layer superlattice (SLS) samples were studied at hydrostatic pressures up to 4.8 GPa at room temperature. A sublinear pressure dependence of the PL peaks for both the heavy-hole exciton and the donor–acceptor pair was observed. The first- and second-order pressure coefficients of the PL peaks were obtained by a least-squares fit. An analytical expression for the heavy-hole exciton was also derived. The pressure coefficients obtained from the analytical expression are 104 meV GPa^{-1} and −4.44 meV GPa^{-2}, in excellent agreement with the experimental values of 103.9 meV GPa^{-1} and −4.5 meV GPa^{-2}. It is shown that the contribution to the linear pressure coefficient comes exclusively from the hydrostatic component. Both hydrostatic and biaxial terms are responsible for the second-order pressure coefficient, with a negative contribution of −6.07 meV GPa^{-2} and a positive contribution of 1.63 meV GPa^{-2}, respectively. Copyright © 2001 John Wiley & Sons, Ltd.

INTRODUCTION

Multiple quantum-well structures and superlattices of II–VI compounds are the subject of intensive study because of their interesting optical properties. Since the demonstration of blue laser action and electroluminescence from ZnSe-based quantum well devices,[1,2] the optical and electrical properties of II–VI semiconductors have attracted considerable attention. Measurements of Photoluminescence (PL) under hydrostatic pressure can be used as a powerful method for the investigation of semiconductor band structure and defect states. Recently, this technique has also been widely employed to study the electronic properties of superlattices and quantum wells. There has been some work on the effects of external pressure modulations in II–VI semiconductors.[3–17] Previously, no high-pressure dependence of PL on $ZnTe/Zn_{1-x}Cd_xTe$ superlattices has been reported. The only publication concerning high-pressure PL on $ZnTe/Zn_{1-x}Cd_xTe$ single quantum wells known to the authors is Ref. 17 for a sample consisting of five thin $Cd_{0.605}Zn_{0.395}Te$ quantum wells separated by 30 nm thick ZnTe barrier layers and a 30 nm thick ZnTe cap layer, where the PL energy exhibits a linear dependence with pressure at low temperature, and the pressure coefficients of the interband transitions decrease with increasing well widths. The PL energies were found to be in excellent agreement with the valence-band offsets calculated by Van de Walle[18] and relative deformation potentials calculated by Christensen and Christensen.[3]

In this paper, we present a study of high-pressure PL on $ZnTe/Zn_{0.77}Cd_{0.23}Te$ superlattices. A sublinear dependence of PL energy with pressure for the heavy-hole exciton of the well layers was observed at room temperature. Theoretical calculations on the pressure coefficients were performed using strain effect theory and comparisons were made between the calculated and experimental results.

EXPERIMENTAL AND RESULTS

The $ZnTe/Zn_{0.77}Cd_{0.23}Te$ SLS samples were grown on a (100)-oriented GaAs substrate at 350 °C by low-pressure metal–organic chemical vapor deposition (LP-MOCVD) with gaseous sources. To minimize the effects due to mismatch with the substrate, a ZnTe buffer layer of about 0.6 μm in thickness was first deposited on the GaAs substrate, followed by 50 periods of 2.5 nm thick $Zn_{0.77}Cd_{0.23}Te$ well layers separated by 5.0 nm thick ZnTe barrier layers. A 30 nm ZnTe layer was grown as the cap layer.

To perform the high-pressure experiments, the GaAs substrate was thinned to about 50 μm thickness and the film was cut into ~80 × 80 μm square samples. The sample was then placed in a gasketed diamond anvil cell (DAC) which was used to generate the hydrostatic pressure. A

*Correspondence to: Z. X. Shen, Department of Physics, Faculty of Science, National University of Singapore, 2 Science Drive 3, Singapore 117542. E-mail: physzx@nus.edu.sg

DOI: 10.1002/jrs.767

JRS

4 : 1 methanol–ethanol mixture was used as the pressure medium. The energy shift of the R1 luminescence line from a ruby chip was used to calibrate the pressure. The PL spectra were recorded with a Spex 1704 spectrograph, equipped with a microscope attachment and CCD detector, and excited by 488 nm radiation from an argon ion laser. The Raman spectral resolution was better than 0.5 cm^{-1}. The power of the laser on the sample was about 2 mW.

ZnTe and $Zn_{1-x}Cd_xTe$ are both direct gap semiconductor materials with a zinc blende structure. In $ZnTe/Zn_{1-x}Cd_xTe$ superlattices, the ZnTe layers experience tensile strain while the $Zn_{1-x}Cd_xTe$ layers are in compression strain, with the strain proportional to the Cd concentration. Figure 1 shows the ambient pressure PL spectra of $ZnTe/Zn_{0.77}Cd_{0.23}Te$ SLS at 77 K and room temperature. The PL spectrum at 77 K exhibits five peaks. The two peaks located at 2.22 and 2.20 eV in the high-energy part of the spectrum at 77 K are attributed to the $n = 1$ light-hole (LH) and heavy-hole (HH) exciton, respectively. The peak located at 2.15 eV in the low-energy part is attributed to the donor–acceptor (D–A) pair recombination. The origin of the other two peaks located at 2.17 and 2.13 eV is not clear. At 300 K, only two peaks, namely HH and D–A, were observable at 2.09 and 2.04 eV, respectively.

The high-pressure PL spectra of $ZnTe/Zn_{0.77}Cd_{0.23}Te$ SLS at room temperature are shown in Fig. 2. Under hydrostatic pressure, the positions of the HH and D–A peaks shift to higher energy and linewidth broadening takes place. The intensity of the PL decreases dramatically above 2.6 GPa.

Figure 3 shows the effect of pressure on the $n = 1$ HH exciton and the D–A pair transition. The emission peaks shift sublinearly to higher energy with increasing pressure. Using least-squares fitting, the PL peak energy is fitted with

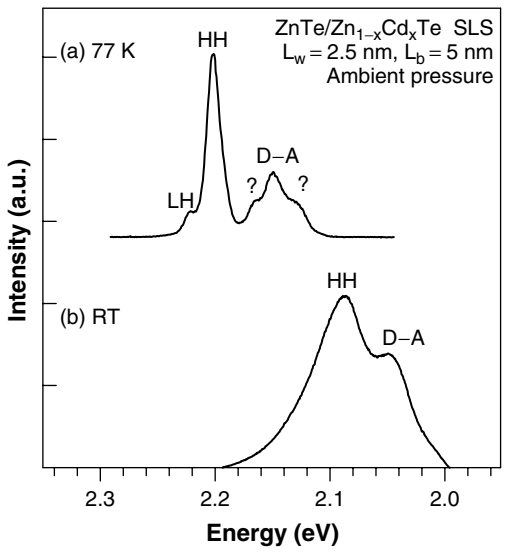

Figure 1. Photoluminescence spectra of $ZnTe/Zn_{0.77}Cd_{0.23}Te$ SLS at (a) 77 K and (b) room temperature.

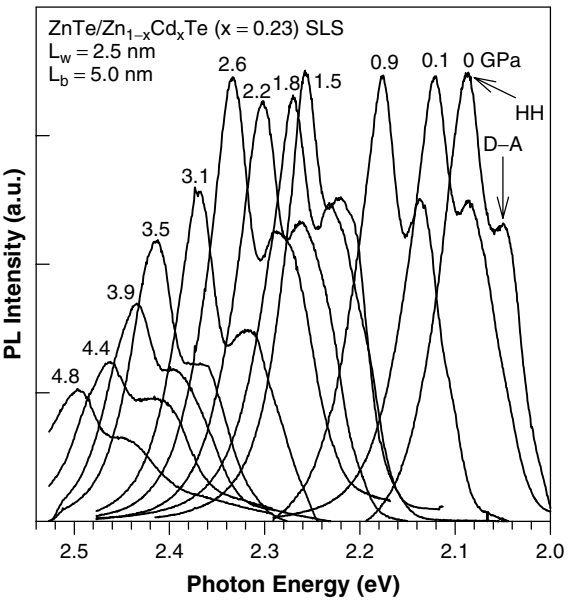

Figure 2. Photoluminescence spectra of $ZnTe/Zn_{0.77}Cd_{0.23}Te$ SLS at room temperature under high pressure as indicated.

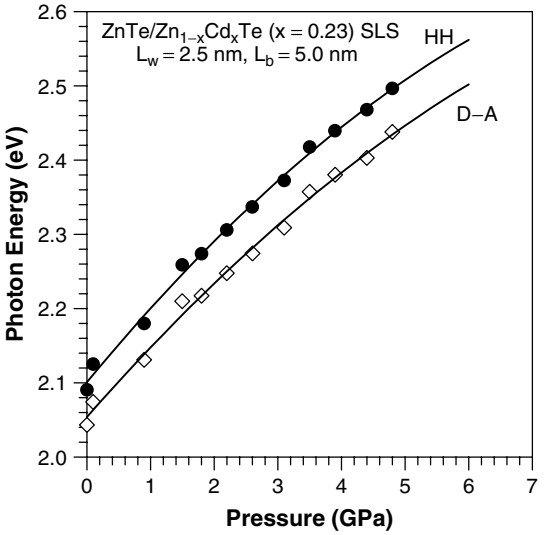

Figure 3. Pressure dependence of the peak energy of the $n = 1$ HH exciton and D–A pair luminescence of the $ZnTe/Zn_{0.77}Cd_{0.23}Te$ SLS at room temperature. The solid lines are the results fitted by the second-order polynomial function.

a second-order polynomial function:

$$E(p) = E(0) + \alpha p + \beta p^2 \quad (1)$$

where $E(0)$ is the inter-band transition energy under atmospheric pressure. The parameters listed in Table 1 are the fitting results.

Analytical expression of PL energy dependence on pressure

In this section, we attempt to derive an analytical expression for the HH exciton transition. The first- and second-order

Table 1. Pressure dependence of the PL peaks obtained using least-squares fitting

	E_0 eV	α/meV GPa^{-1}	β/meV GPa^{-2}
HH	2.1	103.88	−4.50
D–A	2.05	97.45	−3.79

pressure coefficients α and β were calculated using this expression and compared with the fitting result in the previous section. The pressure dependence of the volume change was first obtained using strains and the expression of the HH exciton energy was then derived.

Pressure dependence of strains and volume change

The ZnTe/$Zn_{0.77}Cd_{0.23}Te$ strained superlattices are composed of two-component materials, ZnTe with bulk modulus B_1 as barrier layers and $Zn_{0.77}Cd_{0.23}Te$ with bulk modulus B_2 as well layers. The pressure-dependent strain in the superlattice can be decomposed into a hydrostatic component $\in_{ij}^{(h)}$ and a biaxial component $\in_{ij}^{(b)}$:[9]

$$\overline{\in}_{ij} = \in_{ij}^{(h)} + \in_{ij}^{(b)} \tag{2}$$

The diagonal component $\in_{ii}^{(h)}$ can be expressed as

$$\in^{(h)}(p) = \in_{xx}^{(h)} = \in_{yy}^{(h)} = \in_{zz}^{(h)} = \frac{a(p) - a_0}{a_0} \tag{3}$$

where $a(p)$ is the lattice constant and a_0 denotes the ambient pressure lattice constant. Using Murnaghan's equation of state,[19] $a(p)$ is given by

$$a(p) = a_0 \left(1 + p\frac{B'}{B}\right)^{-1/3B'} \tag{4}$$

where p is pressure, B is the bulk modulus and $B' = \mathrm{d}B/\mathrm{d}p$. At the low-pressure limit, Eqn (4) reduces to

$$a(p) = a_0 \left(1 - \frac{p}{3B}\right) + \frac{B' + 1/3}{6B^2} p^2 \tag{5}$$

Substituting Eqn (5) into Eqn (3), the hydrostatic strain is then given by

$$\in_{xx}^{(h)} = \in_{yy}^{(h)} = \in_{zz}^{(h)} = -\frac{p}{3B} + \frac{B' + 1/3}{6B^2} p^2 \tag{6}$$

The diagonal biaxial strain $\in_{ii}^{(b)}$ can be expressed as

$$\in^{(b)}(p) = \in_{xx}^{(b)} = \in_{yy}^{(b)} = \frac{a_{\mathrm{eq}}(p) - a(p)}{a(p)} \tag{7}$$

$$\in_{zz}^{(b)} = -\frac{2C_{12}}{C_{11}} \in_{xx}^{(b)} \tag{8}$$

where C_{11} and C_{12} are the elastic constants and a_{eq} is the weighted average, in-plane lattice constant for the heterostructures. For ZnTe/$Zn_{1-x}Cd_xTe$ SLS, a_{eq} is given by[9]

$$a_{\mathrm{eq}}(p) = \frac{(a_1 t_1 + a_2 t_2)}{(t_1 + t_2)} \tag{9}$$

where t_1 is the total thickness of all the ZnTe layers in the SLS, including the buffer and cap layers, and t_2 is that of $Zn_{0.77}Cd_{0.23}Te$; a_1 and a_2 are the lattice constants of the ZnTe and $Zn_{0.77}Cd_{0.23}Te$ layers, respectively.

Substituting Eqns (5) and (9) into Eqn (7) and keeping only to the second-order term, the biaxial stain becomes

$$\in^{(b)}(p) = \frac{a_{\mathrm{eq}}}{a}\left\{1 + \frac{p}{3}\left(\frac{1}{B} - \frac{1}{B_{\mathrm{eq}}}\right) + \frac{p^2}{18}\left[\frac{3B'_{\mathrm{eq}} + 1}{B_{\mathrm{eq}}^2} - \frac{3B' + 1}{B^2} + \frac{2}{B}\left(\frac{1}{B} - \frac{1}{B_{\mathrm{eq}}}\right)\right]\right\} - 1 \tag{10}$$

where B_{eq} is the effective bulk modulus and $B'_{\mathrm{eq}} = \mathrm{d}B_{\mathrm{eq}}/\mathrm{d}p$,

$$\frac{1}{B_{\mathrm{eq}}} = \left(2\frac{a_1}{a_{\mathrm{eq}}} - 1\right)\frac{t_1}{t_1 + t_2}\frac{1}{B_1} + \left(2\frac{a_2}{a_{\mathrm{eq}}} - 1\right)\frac{t_2}{t_1 + t_2}\frac{1}{B_2} \tag{11}$$

Using Eqns (2)–(10), the fractional change in volume Ω can be written as

$$\begin{aligned}\frac{\Delta\Omega}{\Omega} &= \overline{\in}_{xx} + \overline{\in}_{yy} + \overline{\in}_{zz} \\ &= \in_{xx}^{(h)} + \in_{yy}^{(h)} + \in_{zz}^{(h)} + \in_{xx}^{(b)} + \in_{yy}^{(b)} + \in_{zz}^{(b)} \\ &= -\frac{p}{B} + \frac{1/3 + B'}{2B^2}p^2 + 2\left(1 - \frac{C_{12}}{C_{11}}\right)\in^{(b)}(p)\end{aligned} \tag{12}$$

The first two terms in the above equation represent the contribution from the hydrostatic component and the last term is the biaxial component.

Pressure dependence of the HH exciton PL peak

For ZnTe/$Zn_{1-x}Cd_xTe$ superlattices, the valence-band energy and the conduction-band energy can be expressed as[18]

$$\Delta E_{\mathrm{v}} = a_{\mathrm{v}}\left(\frac{\Delta\Omega}{\Omega}\right) - b\left[\in_{zz}^{(b)} - \in_{xx}^{(b)}\right] \tag{13}$$

$$\Delta E_{\mathrm{c}} = a_{\mathrm{c}}\left(\frac{\Delta\Omega}{\Omega}\right) \tag{14}$$

where a_{c} and a_{v} are conduction-band and valence-band hydrostatic deformation, respectively, and b is the tetragonal deformation.

Using Eqns (13) and (14), the HH exciton energy can be expressed as

$$\begin{aligned}E &= E_0 + \Delta E_{\mathrm{c}} - \Delta E_{\mathrm{v}} \\ &= E_0 + (a_{\mathrm{c}} - a_{\mathrm{v}})\frac{\Delta\Omega}{\Omega} + b\left[\in_{zz}^{(b)} - \in_{xx}^{(b)}\right] \\ &= E_0 - \frac{a_{\mathrm{c}} - a_{\mathrm{v}}}{B}p + \frac{(a_{\mathrm{c}} - a_{\mathrm{v}})(1/3 + B')}{2B^2}p2 \\ &\quad + [\gamma(a_{\mathrm{c}} - a_{\mathrm{v}}) - b\eta]\in^{(b)}(p)\end{aligned} \tag{15}$$

where the second-order terms, involving $\in p$ and $\in^2$, are small and have been neglected, and

$$\gamma = 2\left(1 - \frac{C_{12}}{C_{11}}\right), \quad \eta = \left(1 + 2\frac{C_{12}}{C_{11}}\right) \tag{16}$$

JRS

Using Eqn (15), the pressure coefficients α and β are given by

$$\alpha = -\frac{a_c - a_v}{B} + \frac{a_{eq}}{3a}\left[\frac{1}{B} - \frac{1}{B_{eq}}\right][\gamma(a_c - a_v) - b\eta] \quad (17)$$

$$\beta = \frac{1/3 + B'}{2B^2}(a_c - a_v) + \frac{a_{eq}}{9a}\left[\frac{3B'_{eq} + 1}{B^2_{eq}} - \frac{3B' + 1}{B^2} + \frac{2}{B}\left(\frac{1}{B} - \frac{1}{B_{eq}}\right)\right] \times [\gamma(a_c - a_v) - b\eta] \quad (18)$$

Hence α and β can be calculated from the material parameters of $Zn_{0.77}Cd_{0.23}Te$ and ZnTe which are listed in Table 2. The first term in the two equations represents the hydrostatic effect and the other terms represent an effect related to the biaxial strain.

The pressure coefficients α and β obtained from the above calculation are 104 meV GPa^{-1} and -4.44 meV GPa^{-2} respectively, in excellent agreement with the values of 103.9 meV GPa^{-1} and -4.5 meV GPa^{-2} derived from our experiment. It is noteworthy that the linear pressure coefficient α comes almost exclusively from the hydrostatic component, which is two orders of magnitude larger than that of the biaxial component. On the other hand, both components are responsible for the second-order pressure coefficient β. The hydrostatic term has a negative contribution of -6.07 meV GPa^{-2} and the biaxial term has a positive contribution of 1.63 meV GPa^{-2}.

Pressure dependence of PL peak intensities

Figure 4(a) and (b) show the pressure dependence of the peak intensity and the linewidth (HWHM) of the $n = 1$ HH exciton emission spectra at room temperature. The solid lines are results of linear least-square fitting to the experimental data. The peak intensity decreases gradually with increasing pressure up to about 2.6 GPa, above which pressure the intensity decreases more rapidly. The pressure dependence of the emission intensity is represented by two straight lines intercepting at about 2.6 GPa. Parallel to the intensity changes, the linewidth shown in Fig. 4(b) increases as the hydrostatic pressure increases, and a kink point also exists in the linewidth–pressure plot at about the same pressure of 2.6 GPa. With increasing pressure, the PL peaks shift to higher energy and close to the excitation source, usually the PL intensity does not show much change before it goes beyond the energy of the excitation source.[21] However, the PL intensity in our experiments decreases dramatically when it is close to the laser line at 2.54 eV.

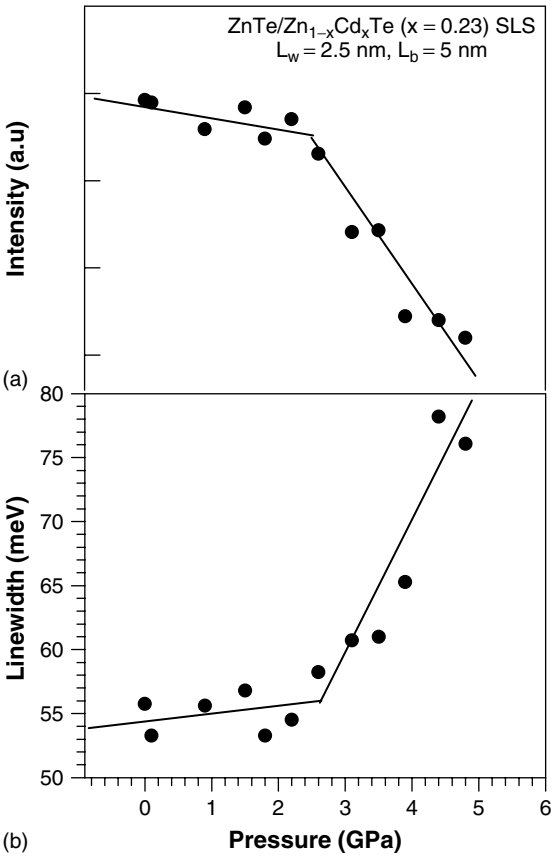

Figure 4. (a) Pressure dependence of the peak intensity and (b) the linewidth of the $n = 1$ HH exciton luminescence peak at room temperature. The solid lines are results of least-squares fitting of the experimental data. Both graphs show a clear gradient change at about 2.6 GPa.

One possible explanation for the abnormal PL intensity behaviour could be that it is due to a structural phase transition. The phase transition pressure of ZnTe is 9.5 GPa.[20] Since the Cd content in the sample is small, the structural properties of the well layers $Zn_{0.77}Cd_{0.23}Te$ are expected to be similar to those of ZnTe. Considering the fact that the $Zn_{0.77}Cd_{0.23}Te$ layers are already under compressive strain, a structural phase transition at 2.6 GPa is a possibility. The observed intensity and linewidth changes could also be due to a pressure-induced type I to type II conversion. At pressures lower than the critical pressure P_c, the

Table 2. Parameters used in calculation in Eqns (17) and (18)[17,20]

	a/nm	$a_c - a_v$/eV	b/eV	$C_{11}/10^{-11}$ Pa^{-1}	$C_{12}/10^{-11}$ Pa^{-1}	B/GPa	B'	n/nm
ZnTe	0.6104	−5.3	−0.92	7.13	4.07	48.0	4.7	880
CdTe	0.6481	−3.33	−1.4	5.33	3.65	42.0	6.4	
$Zn_{0.77}Cd_{0.23}Te$	0.6191	−4.85	−1.03	6.72	3.97	46.6	5.1	125

electrons are confined in the lowest Γ-like conduction-band well in the $Zn_{0.77}Cd_{0.23}Te$ layers, giving rise to a type I transition. At pressures higher than P_c the lowest Γ-like conduction-band minimum and the highest Γ-like valence-band maximum occur in different SL layers: the electron wavefunction is mainly confined in the ZnTe layers whereas the hole wavefunction remains confined in the $Zn_{0.77}Cd_{0.23}Te$ layers. In this case the PL peak corresponds to a type II recombination, which is indirect in real space, occurring across the interface (in k space the transition is still direct), resulting in the drastic decrease of the PL emission intensity. In addition to the intensity changes, the linewidth of the HH PL peak [Fig. 4(b)] remains constant up to 2.6 GPa, and with further compression the linewidth increases rapidly. The same phenomenon was also observed in ZnSe/ZnS, and $ZnSe/ZnS_{0.18}Se_{0.82}$.[14,15]

CONCLUSION

$ZnTe/Zn_{0.77}Cd_{0.23}Te$ SLS samples were studied under hydrostatic pressure. A sublinear pressure dependence of the PL peaks for both the HH and D–A transitions was observed. An analytical expression of the pressure coefficients of the HH PL peak was derived and the results obtained using this expression gave excellent agreement with experiment. The hydrostatic component was shown to be solely responsible for the linear pressure coefficient while both the hydrostatic and biaxial components contribute to the second-order pressure coefficient. The intensity and linewidth of the HH PL peak show a kink at 2.6 GPa.

REFERENCES

1. Haase MA, Qiu J, Depuydt JM, Cheng H. *Appl. Phys. Lett.* 1991; **59**: 1272.
2. Jeon H, Ding J, Patterso W, Nurmikko AV, Xie W, Grillo DC, Kobayashi M, Gunshor RL. *Appl. Phys. Lett.* 1991; **59**: 3619.
3. Christensen NE, Christensen OB. *Phys. Rev. B* 1986; **33**: 4739.
4. Dunstan DJ, Gil B, Homewood KP. *Phys. Rev. B* 1988; **38**: 7862.
5. Shan W, Hays JM, Yang XH, Song JJ. *Appl. Phys. Lett.* 1992; **60**: 736.
6. Jiang S, Shen SC, Li D, Ju YQ, Zhu HR, Schilz J. *Appl. Phys. Lett.* 1992; **60**: 3171.
7. Thomas RJ, Chandrasekhar HR, Chandrasekhar M, Samarth N, Luo H, Furdyna J. *Phys. Rev. B* 1992; **45**: 9505.
8. Tuchman JA, Kim S, Feng ZF, Herman IP. *Phys. Rev. B* 1992; **46**: 13371.
9. Tuchman JA, Sui ZF, Kim S, Herman IP. *J. Appl. Phys.* 1993; **73**: 7730.
10. Hwang SJ, Shan W, Song JJ. *Appl. Phys. Lett.* 1994; **64**: 2267.
11. Thomas RJ, Boley MS, Chandrasekhar HR, Chandrasekhar M. *Phys. Rev. B* 1994; **49**: 2181.
12. Li WS, Chi YB, Li YM, Fan XW, Yang BJ, Shen DZ, Lu YM. *Thin Solid Films* 1995; **266**: 307.
13. Andre R, Cibert J, Dang LS, Zeman J, Zigone M. *Phys. Rev. B* 1996; **53**: 6951.
14. Yamada Y, Masumoto Y, Taguchi T, Takemura K. *Phys. Rev. B* 1990; **44**: 1801.
15. Gorczyca I, Christensen NE. *Phys. Rev. B* 1993; **48**: 17 202.
16. Baugher EM, Chandrasekhar M, Chandrasekhar HR, Luo H, Furdyna JK, Ram-Mhan LR. *J. Phys. Chem. Solids* 1995; **56**: 323.
17. Pelhos K, Lee SA, Rajakarunanayake Y, Reno JL. *Phys. Rev. B* 1995; **51**: 13256.
18. Van de Walle CG. *Phys. Rev. B* 1989; **39**: 1871.
19. Murnaghan FD. *Proc. Natl. Acad. Sci. USA* 1944; **30**: 244.
20. Tuchman JA, Herman IP. *Phys. Rev. B* 1992; **45**: 11 929.
21. Li WS, Shen ZX, Shen DZ, Fan XW. *J. Appl. Phys.* 1998; **84**: 5198.